AD-A032 993 AEROSPACE CORP EL SEGUNDO CALIF F/G 4/1
A CONTROLLED VLF PHASE-REVERSAL EXPERIMENT IN THE MAGNETOSPHERE--ETC(U)
NOV 76 H C KOONS, M H DAZEY, R L DOWDEN F04701-76-C-0077
UNCLASSIFIED TR-0077(2960-02)-1 SAMSO-TR-76-218 NL

| OF |

AD
A032993

END
DATE
FILMED
1 -77

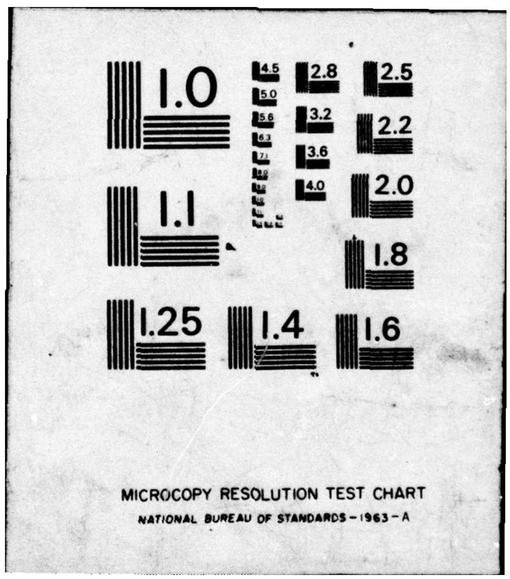
1.0
1.1
1.25
1.4
1.6
1.8
2.0
2.2
2.5
2.8
3.2
3.6
4.0
4.5
5.0
5.6
6.3
MICROCOPY RESOLUTION TEST CHART
NATIONAL BUREAU OF STANDARDS-1963-A

REPORT SAMSO-TR-76-218

ADA032993

(12)

A Controlled VLF Phase-Reversal Experiment in the Magnetosphere

Space Sciences Laboratory
The Ivan A. Getting Laboratories
The Aerospace Corporation
El Segundo, Calif. 90245
and
Department of Physics
University of Otago
Dunedin, New Zealand

4 November 1976

Interim Report

APPROVED FOR PUBLIC RELEASE;
DISTRIBUTION UNLIMITED

Prepared for
SPACE AND MISSILE SYSTEMS ORGANIZATION

This report was submitted by The Aerospace Corporation, El Segundo, CA 90245, under Contract F04701-75-C-0076 with the Space and Missile Systems Organization, Deputy for Advanced Space Programs, P.O. Box 92960, Worldway Postal Center, Los Angeles, CA 90009. It was reviewed and approved for The Aerospace Corporation by G. A. Paulikas, Space Sciences Laboratory. Lieutenant Jean Bogert, SAMSO/YAPT, was the project engineer.

This report has been reviewed by the Information Office (OI) and is releasable to the National Technical Information Service (NTIS). At NTIS, it will be available to the general public, including foreign nations.

This technical report has been reviewed and is approved for publication. Publication of this report does not constitute Air Force approval of the report's findings or conclusions. It is published only for the exchange and stimulation of ideas.

FOR THE COMMANDER

Jean Bogert

Jean Bogert, 1st Lt, USAF
Technology Plans Division
Deputy for Advanced Space
Programs

UNCLASSIFIED

SECURITY CLASSIFICATION OF THIS PAGE (When Date Entered)

(19) REPORT DOCUMENTATION PAGE		READ INSTRUCTIONS BEFORE COMPLETING FORM
1. REPORT NUMBER (18) SAMSO TR-76-218	2. GOVT ACCESSION NO.	3. RECIPIENT'S CATALOG NUMBER
4. TITLE (and Subtitle) (6) A CONTROLLED VLF PHASE-REVERSAL EXPERIMENT IN THE MAGNETOSPHERE.		5. TYPE OF REPORT & PERIOD COVERED (9) Interim rept.,
		6. PERFORMING ORG. REPORT NUMBER (14) TR-0077(2960-02)-1
7. AUTHOR(s) (10) H. C. Koons, M. H. Dazey, R. L. Dowden and L. E. S. Amon		8. CONTRACT OR GRANT NUMBER(s) (15) F04701-76-C-0077
9. PERFORMING ORGANIZATION NAME AND ADDRESS The Aerospace Corporation El Segundo, Calif. 90245		10. PROGRAM ELEMENT, PROJECT, TASK AREA & WORK UNIT NUMBERS (12) 31p.
11. CONTROLLING OFFICE NAME AND ADDRESS Space and Missile Systems Organization Air Force Systems Command Los Angeles, Calif. 90009		12. REPORT DATE (11) 4 Nov[redacted]76
		13. NUMBER OF PAGES 31
14. MONITORING AGENCY NAME & ADDRESS(if different from Controlling Office)		15. SECURITY CLASS. (of this report) Unclassified
		15a. DECLASSIFICATION/DOWNGRADING SCHEDULE

16. DISTRIBUTION STATEMENT (of this Report)

Approved for public release; distribution unlimited

17. DISTRIBUTION STATEMENT (of the abstract entered in Block 20, if different from Report)

18. SUPPLEMENTARY NOTES

19. KEY WORDS (Continue on reverse side if necessary and identify by block number)

Magnetosphere
Very-Low-Frequency Propagation
Wave-Particle Interactions
Whistler Mode

20. ABSTRACT (Continue on reverse side if necessary and identify by block number)

During the 1973 operations of the transportable very-low-frequency (TVLF) transmitter near Anchorage, Alaska (L ~ 4), an experiment was performed to determine the effect of controlled phase changes of the transmitted wave on the magnetospherically propagated signal received in the conjugate region. At periodic intervals, the phase of the driving voltage was changed (essentially instantaneously) by 180°. The amplitude of the 6.6 kHz signal detected in the conjugate region went to zero and recovered with a characteristic time

next page

DD FORM 1473 (FACSIMILE)

deg

009 508

UNCLASSIFIED

SECURITY CLASSIFICATION OF THIS PAGE (When Date Entered)

UNCLASSIFIED

SECURITY CLASSIFICATION OF THIS PAGE(When Data Entered)

19. KEY WORDS (Continued)

20. ABSTRACT (Continued)

cont.

constant of 33 msec. This is ten times longer than the antenna current response time and is in fact comparable with characteristic electron interaction times with whistler-mode waves. Between the times at which the phase reversals occurred, the received signal was amplitude modulated. The period of the modulation was about ~~1~~26 msec. An upper sideband was present in the spectrum while these pulsations were occurring. These characteristic times are in general agreement with theoretical predictions of bandwidths, growth rates, and particle trapping frequencies for whistler instabilities in the magnetosphere. Data obtained from the controlled transmissions and from lightning generated whistlers propagating in the same duct were combined to determine the plasma and wave parameters at the geomagnetic equator. Of particular interest is the level at which the magnetic field of the wave saturated. During the time period for which the data were analyzed, this was found to be 3.5 pT. ~~(my).~~

UNCLASSIFIED

SECURITY CLASSIFICATION OF THIS PAGE(When Data Entered)

PREFACE

It is a pleasure to acknowledge productive discussions with M. Schulz. We are grateful to Lynn Friesen for the computer calculations. This work was supported in part by the National Science Foundation under Grant GA-37730 and in part by the U.S. Air Force Space and Missile Systems Organization (SAMSO) under contract F04701-75-C-0076.

CONTENTS

TABLE

FIGURES

FIGURES (Continued)

INTRODUCTION

Theoretical models and computer simulations of the interaction between narrow-band, whistler-mode waves and energetic electrons using parameters suitable to the magnetosphere show that the resonant electrons are phase-bunched by the waves [e.g. Brinca, 1972; Helliwell and Crystal, 1973; Nunn, 1974]. In a monochromatic wave, the motion of an electron is determined by the force acting on the particle from the electric and magnetic fields of the wave. A feedback loop is established between the radiation emitted by the phase-bunched electrons and the resonant electrons entering the interaction region. The dominant force is the magnetic force which causes a longitudinal drift of the electrons, i.e. a drift along the geomagnetic field line.

If θ is the angle between the electron velocity component $v_\perp$ perpendicular to the magnetic field and the magnetic field component B_w of the wave, the longitudinal drift produces an effective phase rotation between $v_\perp$ and B_w. This phase rotation changes the force responsible for the longitudinal drift. The "equation of motion" for the angle θ is [Helliwell and Crystal, 1973]

$$d^2\theta/dt^2 + \left(\frac{q}{m}\right) k\, v_\perp\, B_w \sin\theta = 0 \tag{1}$$

This is the same form as the equation for the anharmonic motion of a simple pendulum.

If the phase of the transmitted wave is changed abruptly, the solution to (1) requires a new initial value for θ established by the phase change of the wave.

Controlled experiments to observe the effect of phase changes of a whistler-mode wave in wave-particle interactions in the magnetosphere were undertaken in conjunction with very-low-frequency (VLF) wave transmission experiments conducted at Fort Richardson, Alaska in the summer of 1973. These experiments were performed with the transportable very-low-frequency (TVLF) transmitter facility [Koons and Dazey, 1974].

Between September 3 and September 14 phase reversal programs were transmitted daily at frequencies of 6.6 kHz and 13.275 kHz. At 13.275 kHz the TVLF transmitter radiates approximately 1000 W. The primary ground-based receiver in the conjugate area was located at Dunedin, New Zealand ($L \sim 3$). At that site, the amplitude of the earth-ionosphere waveguide signal at 13.275 kHz was typically 10 to 20 μV/m. For cw type transmissions this made it difficult to separate the magnetospheric signal from the waveguide signal which was typically a few μV/m. At 6.6 kHz the radiated power was 100 W. With the increased attenuation at the lower frequency, the waveguide signal was generally below the receiver sensitivity. The data discussed below were obtained during transmissions at 6.6 kHz.

INSTRUMENTATION

The TVLF transmitter is a linear, Class AB, power amplifier driven by a low-voltage, highly-stable, frequency synthesizer. A block diagram of the transmitter and control circuit including the phase reversal switch is shown in Figure 1. Frequency stability is provided by a 5 MHz quartz crystal oscillator in the frequency synthesizer which generates the 6.6 kHz signal for the transmitter. The stability of the oscillator is ± 1 part in 10^8 per day. A 1 MHz signal derived from the 5 MHz oscillator also drives a time-code generator. The time-code generator is set within ± 2 msec of Universal Time by synchronization of a 1 pulse-per-second output with the second marks transmitted by the Time Standard Station WWVH. Proper account was taken of the propagation delay from WWVH to the TVLF transmitter site.

An identical frequency synthesizer at the receiver site in New Zealand was synchronized with the Australian Time Standard Station VNG. The time code recorded at the receiver site was also maintained within ± 2 msec of Universal Time and the overall system timing accuracy was ± 4 msec.

At periodic intervals phase inversion (180° phase shifts) of the driving voltage is achieved by a COSMOS integrated circuit reversing switch that is keyed by a programmer driven by the time-code generator. The switch accomplishes the phase reversal in about 1 μsec. It can be keyed 32, 16, 8, 4, 2, 1, 0.5, 0.2, 0.1, 0.0333..., or 0.01666... times per second. The signal out of the switch passes through a unity gain differential amplifier, an audio amplifier and finally provides the input

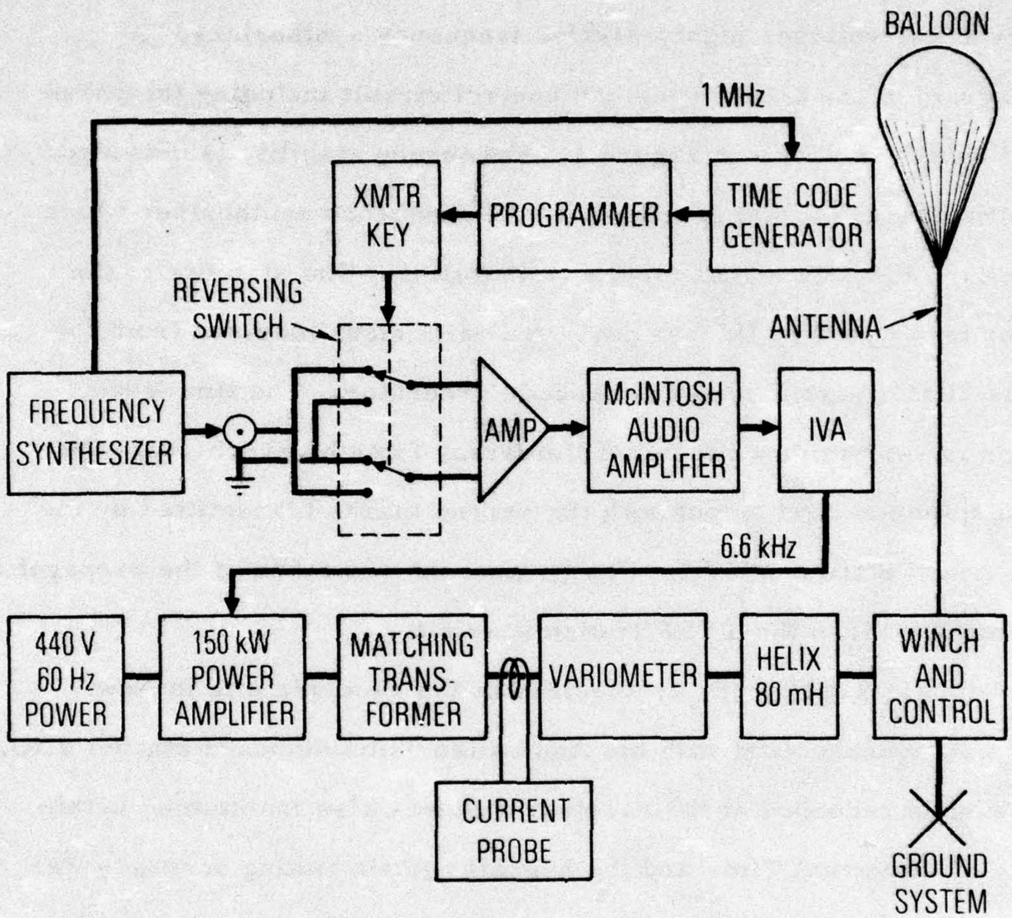

Fig. 1 **Block diagram of the TVLF transmitter system.**

signal to the Intermediate Voltage Amplifier of the transmitter.

The main instrumental effect attributed to the transmitter is the rise time of the tuning circuit. The antenna system is essentially a series RLC circuit fed by a matching transformer. The circuit is shown in Figure 1. The current to the antenna is measured by a calibrated current probe on the output side of the matching transformer. The Q of the circuit was periodically measured by sweeping the transmitter frequency about the center frequency and measuring the bandwidth at 0.707 of the maximum current. About 25 minutes after the phase reversal transmissions discussed below, the Q was measured to be 68 which corresponds with a current rise time of 3.3 msec.

OBSERVATIONS

On September 6, 1973 strong whistler-mode signals from the transmitter were detected at 6.6 kHz. During a 20-sec period centered at 21:43:30 Universal Time, strong signals were detected while a phase reversal program was being transmitted. The signal amplitude averaged over a 10-sec period was 18 $\mu V/m$. The noise in a 50 Hz bandwidth at 6500 Hz was 3 $\mu V/m$. During this time period, phase reversals were keyed at 0.5 sec intervals. Figure 2 shows a record of the signal amplitude as a function of time. During that time period the amplitude of the received signal gradually increased 10 db, then returned to its previous level.

In Figure 2 it can be seen that the signal amplitude periodically decreases in amplitude and then recovers. This occurs every 0.5 sec which is the time interval at which the 180^{o} phase shifts were being applied to the transmitted signal.

In Figure 3 a short section of the amplitude record is reproduced with higher time resolution together with a measurement of the phase of the received signal. The phase measurement shows an abrupt phase discontinuity of 180^{o} each time the amplitude goes through a minimum. These measurements demonstrate that phase coherence is maintained throughout the magnetospheric propagation path.

In Figure 3 a sinusoidal amplitude modulation is also apparent particularly in the signal at 12:43:34 UT. Most of the record is contaminated by impulsive sferics. However, no sferics were apparent in the data during the 0.5 sec time period between the phase reversals which straddle 12:43:34 UT.

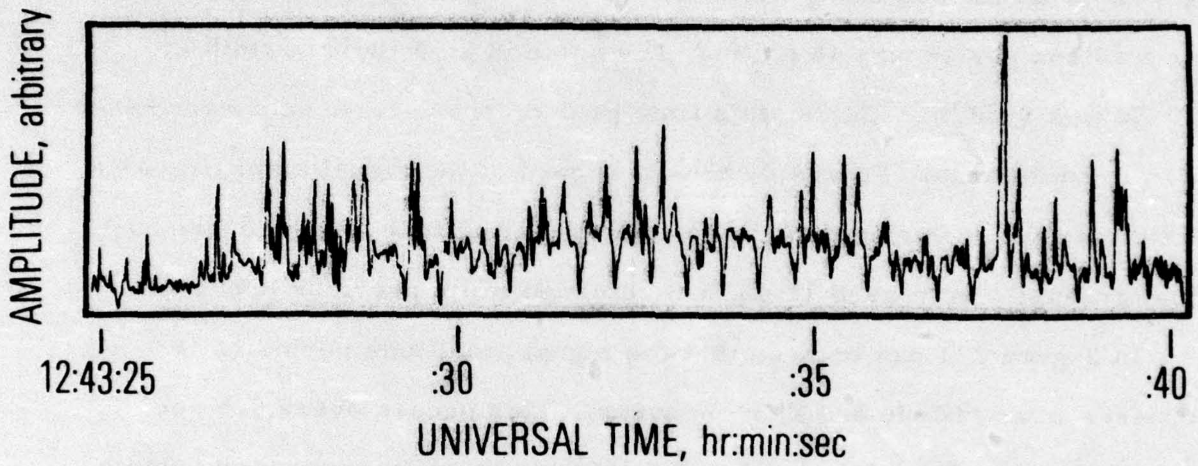

Fig. 2 Amplitude of the 6.6 kHz signal received at Dunedin, New Zealand as a function of time during a period when the transmitter was sending a program in which the phase of the voltage driving the power amplifier was reversed at 0.5 sec intervals. The amplitude scale is linear in magnetic field intensity.

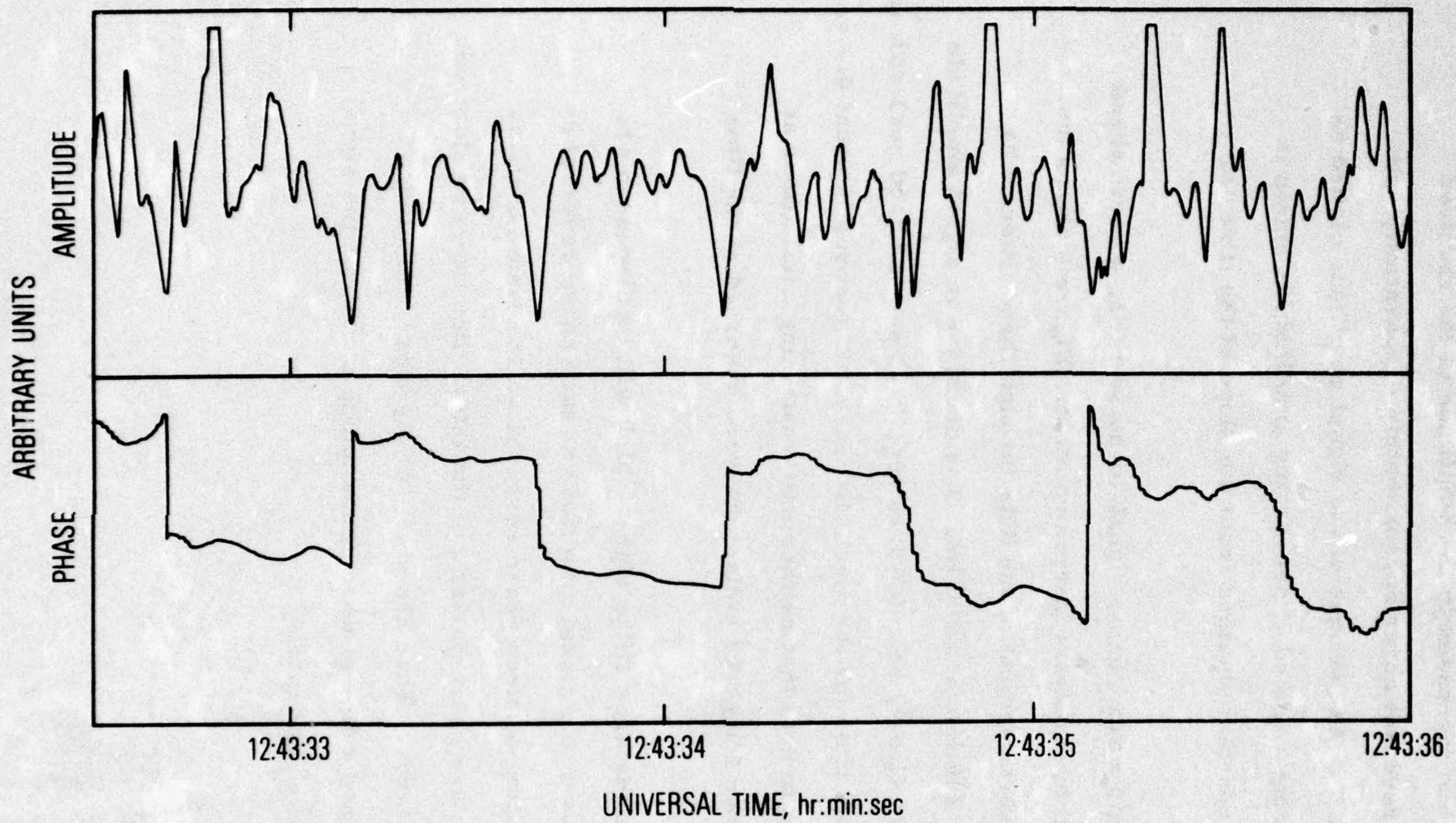

Fig. 3 Amplitude (top) and phase (bottom) of the signal received at a time period near the time of maximum amplitude of the data shown in Fig. 2. The amplitude scale is linear in magnetic field intensity. The measured phase discontinuities shown in the bottom segment are 180°.

The decreases and increases in the amplitude of the received signal at each phase reversal occur approximately exponentially with equal time constants, τ . An example of the signal amplitude plotted as a function of time during a period of decreasing amplitude is shown in Figure 4. The time constant obtained from the slope of the line is 33 msec.

In order to obtain a reasonable signal-to-noise ratio, a narrowband filter was required in the analysis instrumentation. Figure 5 shows the result of passing a short segment of the data through three filters with bandwidths of 80 Hz, 240 Hz, and 800 Hz. The decrease in signal amplitude at 0.5 sec intervals is clearly seen (at 0.13 sec, 0.63 sec and 1.13 sec) with all three filters. The total time for the signal to decay and recover is about 0.1 sec.

It is interesting to note that neither self-sustaining oscillations at the previous phase, nor triggered emissions were observed at the time of a phase reversal.

Two distinctive features of the signal which will be discussed are the rise and fall times of the signal amplitude at each phase reversal and the amplitude modulation between phase reversals. The time constants and periods observed are characteristic of the interaction times of electrons with whistler-mode waves. They are significantly longer than those associated with the bandwidths of the antenna tuning circuit or the signal analysis instrumentation circuits.

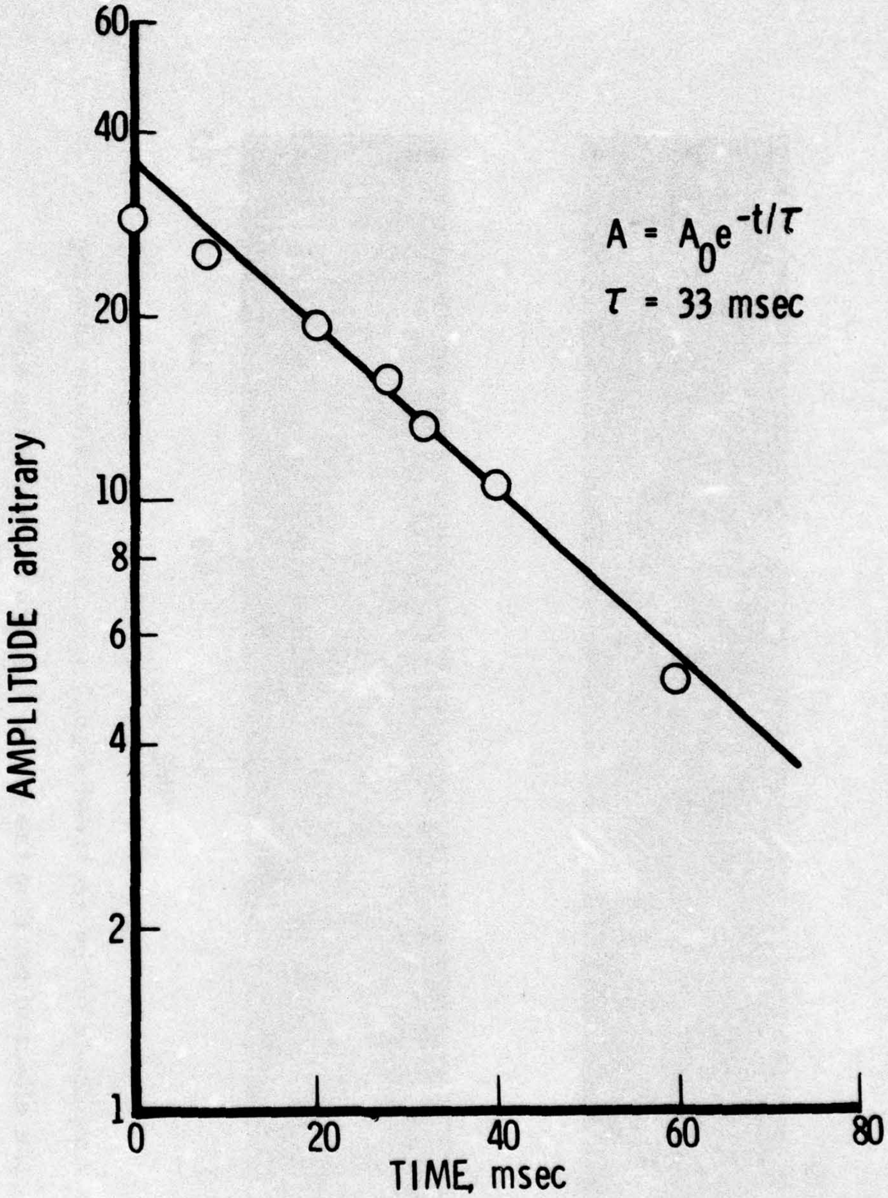

Fig. 4 Amplitude of the received signal as a function of time during a signal decrease following a phase reversal.

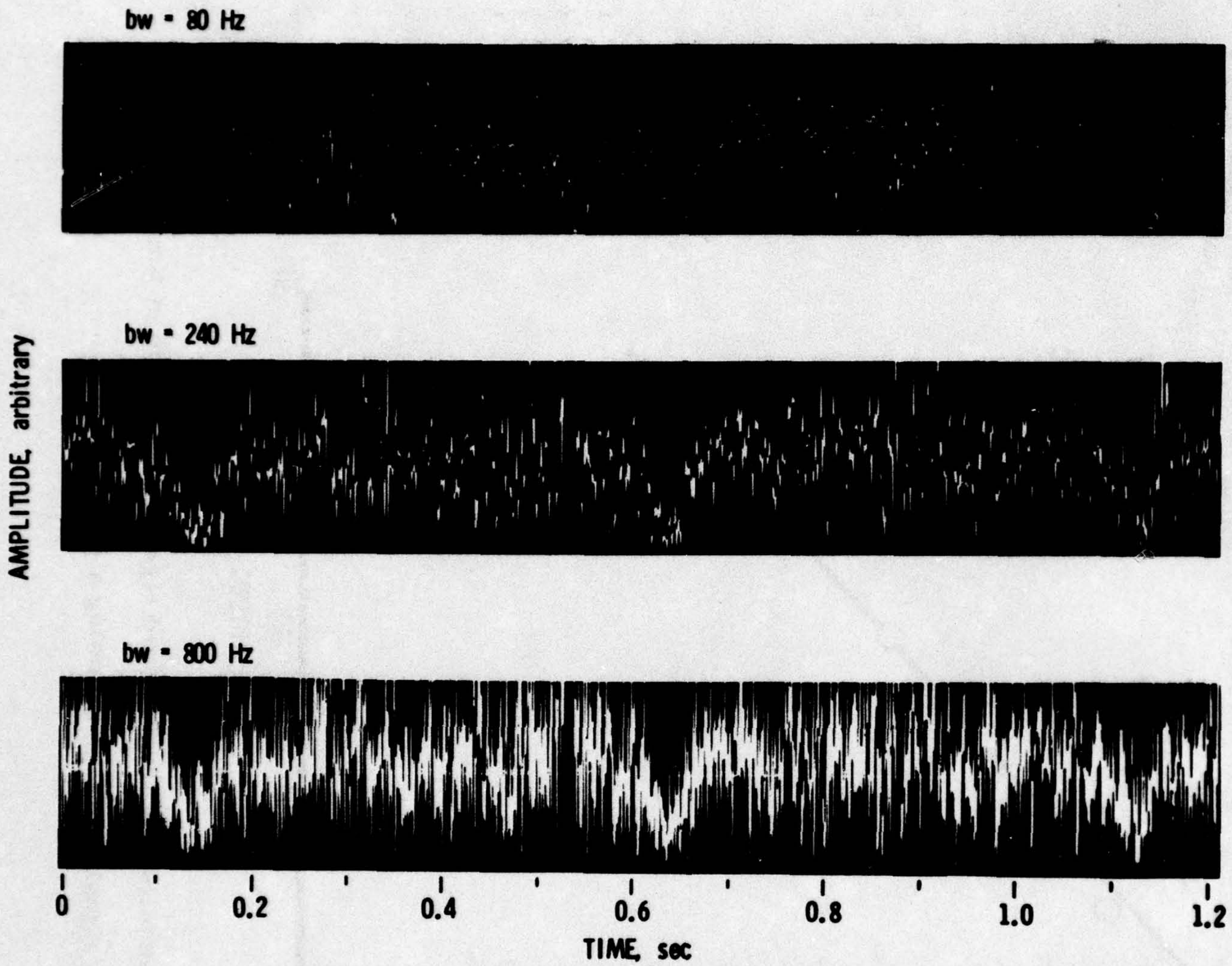

Fig. 5 Amplitude of the received signal as a function of time showing the effect of passing the signal through three filters with bandwidths of 80 Hz, 240 Hz, and 800 Hz. The amplitude scale is linear in magnetic field intensity.

DISCUSSION

Interaction Bandwidth. The decrease and subsequent increase of the signal amplitude at each phase reversal is analogous to the response of a resonant RLC electric circuit when the phase of an applied sinusoidal voltage at the resonant frequency, $\omega^* = 1 / \sqrt{LC}$, is reversed. In the electrical circuit the decay time τ^* for the amplitude is related to the Q of the circuit and to the bandwidth, $\Delta\omega^* / 2\pi$ by

$$Q = \omega^* \tau^* / 2 = \omega^* / \Delta\omega^* \tag{2}$$

This bandwidth arises from the dissipation of the energy by ohmic heating in the resistive components of the circuit.

In the VLF phase reversal experiment, the decay time for the wave amplitude following a phase reversal is measured to be 33 msec. For this time constant, the effective Q obtained from (2) is 684 and the bandwidth, $\Delta\omega^* / 2\pi$, is 9.6 Hz. Several "dissipation" processes influence the effective bandwidth in the resonant wave-particle interaction. Among them are Landau damping, phase mixing in the non-uniform magnetic field, and radiation.

Schulz [1972, 1974] has derived the following expression for the intrinsic bandwidth of cyclotron resonance in a non-uniform magnetic field

$$\Delta\omega / 2\pi = |(\ddot{\omega}/16\pi)|^{1/3} [1 - v_{\parallel}/v_g)]^{-2/3} \tag{3}$$

where

$$\ddot{\omega} = v_{\parallel} \frac{d}{ds} \left(v_{\parallel} \frac{d\omega}{ds} \right) \tag{4}$$

where s is the arc length along the field line and ω is evaluated at the equator (s = o), $v_{\parallel} = \vec{v} \cdot \hat{B}$, and $v_g \equiv d\omega/dk_{\parallel}$.

For the plasma parameters appropriate to the phase reversal experiment (see below) the intrinsic bandwidth is calculated to be 26 Hz.

One must be cautious in comparing this with the observed value. The intrinsic bandwidth calculated by Schulz [1972, 1974] includes only the effect of the non-uniform magnetic field on the bandwidth. Other effects such as wave growth (which would tend to increase $\Delta\omega$) and phase trapping (which would tend to decrease $\Delta\omega$) could alter the actual bandwidth from this "intrinsic" bandwidth.

Amplitude Modulation. Amplitude modulated whistler-mode signals from VLF transmitters have previously been reported by Likhter et al. [1971] and Bell and Helliwell [1971]. This modulation is believed to occur at approximately the phase bunching frequency of the electrons which are undergoing pendulum-type motion in the potential well of the wave [Brinca, 1972; Nunn, 1974, 1975]. However, Helliwell and Crystal [1975] point out that the amplitude pulsations are a fundamental result of the feedback in their model and not a consequence of the oscillatory electron motion due to the phase bunching.

The modulation period scaled from the TVLF experiment data between 12:43:33.65 UT and 12:43:34.15 UT shown in Figure 3 is greater than the actual period because the signal was passed through a 10 Hz filter to produce that display. The modulation period was determined by measuring the frequency offset of the sideband responsible for the modulation. For this purpose, maximum entropy spectrum analysis was applied to a 250 msec interval of the data. The beginning of the interval was 12:43:33.69 UT. The data were sampled at 25,000 samples per second. The program developed by Ulrych and Bishop [1975] to evaluate the Burg estimates of the autoregressive coefficients was used for the spectral determination

Since the maximum entropy spectrum is an optimally smoothed one, Ulrych and Bishop [1975] conclude that the resolution of the Burg maximum entropy method spectrum is almost twice that of a periodogram spectrum [Radoski et.al., 1975].

The power spectral density for the TVLF data using 1000 coefficients is plotted in Figure 6. The points are plotted at one Hertz intervals. The

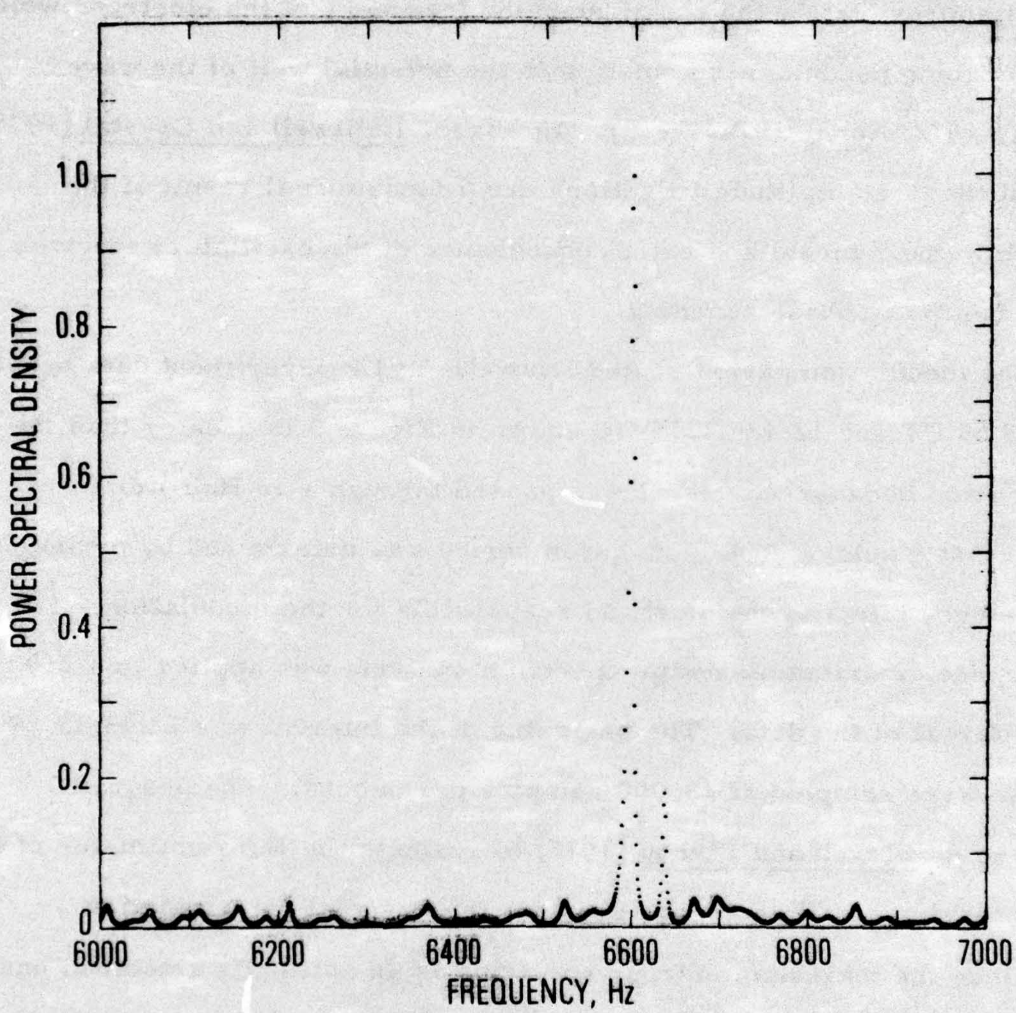

Fig. 6 **Burg maximum entropy spectrum, with 1000 coefficients, of the VLF signal during the amplitude pulsations at 12:43:34 UT.**

dominant peak occurs at the TVLF carrier frequency with a maximum at 6599 Hz. The offset from 6600 Hz is attributed to an imperfect lockup with the reference frequency during digitization. An upper sideband with a maximum at 6638 Hz is also present in the spectrum [Brinca, 1972].

The difference frequency between the carrier and the sideband is 39 Hz. The corresponding modulation period would be 26 msec. The total power in the carrier obtained by integrating the spectral density over the peak is 6.2 times the total power in the sideband.

Amplitude Saturation. Ossakow et al. [1972] have presented the results of computer simulation studies of whistler instabilities in anisotropic, collision-less plasmas. They argue that wave growth saturates when the bounce frequency of a particle in the potential minimum of the wave becomes of the order of the linear growth rate, $\tilde{\omega} \sim \gamma$, where $\tilde{\omega}$ is the particle bounce (or "trapping") frequency given by $\tilde{\omega} = 2\pi/T$ and γ is the linear growth rate. The computer simulation study of Ossakow et al. [1972] yielded the saturation condition

$$\gamma = a\,\tilde{\omega} \tag{5}$$

where, for bi-Maxwellian distribution functions, a is a number between 0.25 and 0.6, and, for two cases with Maxwellian distribution functions with a loss cone, a is 0.2 and 0.25. For a case representative of the magnetospheric plasma [Ossakow et al., 1973] $a = 0.2$. For the computer simulations, they define a discreteness parameter $d = \gamma / k \Delta V_{res}$ where k is a quantized wave number, and ΔV_{res} is the interval between two discrete adjacent resonant velocities. When $d \simeq 1$, then a particle is only in resonance with one wave at a time. This is the condition required to simulate an interaction between the electrons and the coherent signal transmitted by the TVLF transmitter. For one of the bi-Maxwellian cases, $d \sim 0.1$ and $\alpha = 0.3$; for the magnetospheric plasma case $d \sim 0.2$ and $\alpha = 0.2$.

If we identify the time constant of the increase in signal amplitude following a phase reversal with the linear growth rate of the wave, we have a measured value of $\gamma = 1/\tau \sim 30 \text{ sec}^{-1}$ (recalling that the time constants of the signal increases and signal decreases are the same). This growth rate is significantly higher than that reported by Helliwell and Katsufrakis [1974]. In comparing our results with those shown in Fig. 4 of Helliwell and Katsufrakis [1974] we also note that the time to reach saturation is three to four times longer in their data than in the current experiment. The two experiments are not entirely comparable because the particle phases, with respect to the magnetic-field vector, are presumed to be random in the experiment described by Helliwell and Katsufrakis, but are organized to an unknown degree in the phase-reversal experiment.

Although there is not general agreement that the modulation period is a direct measure of the phase bunching period [Nunn, 1975; Helliwell and Crystal, 1975] we will assume that it is and take the radian frequency of the modulation for the phase bunching frequency, $\tilde{\omega} = 2\pi/T = 245 \text{ sec}^{-1}$. Then, the value for α obtained from the TVLF transmission experiment is 0.12.

Again, one must be cautious in comparing the results of the TVLF measurements with the computer simulation. The characteristic plasma parameters, listed in Table 1, differ considerably. Also, some degree

Table 1. Comparison of parameters (ω_p, plasma frequency, and ω_c, cyclotron frequency) in the computer simulation study and the TVLF phase reversal experiments.

Computer Simulation	TVLF Experiment
$\omega \sim 0.7\ \omega_c$	$\omega \sim 0.23\ \omega_c$
$\omega_p = \omega_c$	$\omega_p \sim 6\ \omega_c$
loss cone = 60^o	loss cone ~ 8^o

of phase coherence existed at the time the phase reversals were applied during the TVLF experiment. Hence, the initial conditions in the two experiments were not alike. To be strictly correct, a simulation is required which includes periodic phase reversals for waves propagating in a plasma in a non-uniform magnetic field.

The magnetic field intensity B_w of the whistler-mode wave at saturation may be estimated if we identify the modulation period obtained from the data from the present experiment with the phase bunching period T given by [Helliwell, 1967]

$$T = \left(\frac{2\pi m \lambda}{q \, v_{\parallel} \, \tan \alpha \, B_w} \right)^{1/2} \tag{6}$$

where m is the mass of the electron, λ is the wavelength of the whistler-mode wave, q is the charge of the electron, $v_{\parallel}$ is the velocity of the resonant electrons parallel to the geomagnetic field, and α is the pitch angle of the electron velocity vector. It is assumed that the wave is propagating parallel to the geomagnetic field.

The plasma density required to evaluate λ and $v_{\parallel}$ can be obtained from single-and multiple-hop, lightning-generated whistlers which were occurring throughout this time period. Propagation through only one duct is apparent in the data. The nose frequency obtained by the nose extension method was 11.1 kHz and the time delay at the nose was 1.05 sec. This places the duct at L = 3.1 for the gyrofrequency electron density model [Helliwell, 1965]. The travel time at 6.6 kHz would be 1.14 sec in good agreement with the delay observed for the arrival of the phase shifts at Dunedin, namely 1.15 sec. The second marks along the axis of abscissas in Fig. 3 are properly positioned at the Universal Time seconds in relation to the data.

The minimum amplitude attained during the phase reversal immediately following the mark at 12:43:34 UT is measured to occur at 12:43:34.15 UT. This phase reversal was transmitted at 12:43:33 UT. The electron density at the equator obtained from the travel time of the whistlers at the nose requency is 345 cm^{-3}. The index of refraction for a 6.6 kHz wave propagating parallel to the geomagnetic field is then 13.8 which yields a wavelength of 3290 m. For these plasma parameters the parallel velocity, $v_{\parallel}$, of an electron which is resonant with the wave through a cyclotron resonance is 7.3×10^{7} m/sec. Helliwell [1967] has shown that the characteristic pitch angle for the interaction is 30^{o}. Since the measurements do not provide this pitch angle, 30^{o} will be adopted for these calculations. Substituting for T, λ, v and α in (6), the value obtained for B_w in the interaction region is 3.5 pT (mγ).

CONCLUSIONS

We have presented the results of a controlled VLF transmission experiment conducted to determine the role played by the phase of a whistler-mode wave in wave-particle interactions.

It is observed that the phase of the signal remains coherent throughout the magnetospheric propagation path to the receiver in the conjugate region of the transmitter.

When periodic phase reversals are applied to the transmitted signal, the response of the magnetosphere is analogous to that of a tuned electric circuit with a bandwidth comparable to bandwidths predicted for cyclotron resonance.

In this experiment the amplitude saturated at a magnetic field intensity of 3.5 pT (mγ). Following a phase reversal, the "linear" growth rate is found to be 0.12 times the phase bunching frequency at saturation.

REFERENCES

Bell, T.F., and R.A. Helliwell, Pulsation phenomena observed in long-duration VLF whistler-mode waves, J. Geophys. Res., 76, 8414, 1971.

Brinca, A.L., Whistler side-band growth due to nonlinear wave-particle interaction, J. Geophys. Res., 77, 3508, 1972.

Helliwell, R.A., A theory of discrete VLF emissions from the magnetosphere, J. Geophys. Res., 72, 4773, 1967.

Helliwell, R.A., Whistlers and Related Ionospheric Phenomena, Stanford University Press, Stanford, California, 1965.

Helliwell, R.A. and T.L. Crystal, Reply (to Nunn, 1975), J. Geophys. Res., 80, 4399, 1975.

Helliwell, R.A. and T. L. Crystal, A feedback model of cyclotron interaction between whistler-mode waves and energetic electrons in the magnetosphere, J. Geophys. Res., 78, 7357, 1973.

Helliwell, R.A. and J.P. Katsufrakis, VLF wave injection into the magnetosphere from Siple Station, Antarctica, J. Geophys. Res., 79, 2511, 1974.

Koons, H.C. and M.H. Dazey, Transportable VLF transmitter, in ELF-VLF Radio Wave Propagation, edited by J. Holtet, D. Reidel Publishing Company, Dordrecht-Holland, 1975.

Likhter, Ya. I., O.A. Molchanov, and V.M. Chmyrev, Modulation of spectrum and amplitude of low-frequency signal in the magnetosphere plasma, Sov. Phys. JETP Lett., 14, 325, 1971.

Nunn, D., A self-consistent theory of triggered VLF emissions, Planet. Space Sci., 22, 349, 1974.

Nunn, D., Comment on 'A feedback model of cyclotron interaction between whistler mode waves and energetic electrons in the magnetosphere' by R.A. Helliwell and T. L. Crystal, J. Geophys. Res., 80, 4397, 1975.

Ossakow, S.L., E. Ott, and I. Haber, Nonlinear evolution of whistler instabilities, Phys. Fluids, 15, 2314, 1972.

Ossakow, S.L., E. Ott, and I. Haber, Theory and computer simulation of whistler turbulence and velocity space diffusion in the magnetospheric plasma, J. Geophys. Res., 78, 2945, 1973.

Radoski, H.R., P. Fougere, and E.J. Zawalick, A comparison of power spectral estimates and applications of the maximum entropy method, J. Geophys. Res., 80, 619, 1975.

Schulz, Michael, Intrinsic bandwidth of cyclotron resonance in the geomagnetic field, Phys. Fluids, 15, 2448, 1972.

Schulz, Michael, Trapping of particles by waves in a non-uniform plasma, in Wave-Particle Interactions in the Magnetospheric Plasma, Aerospace Report No. ATR-74 (7420)-1, edited by Michael Schulz, The Aerospace Corporation, El Segundo, California, 1974.

Ulrych, Tad J. and Thomas N. Bishop, Maximum entropy spectral analysis and autoregressive decomposition, Rev. Geophys. Space Phys., 13, 183, 1975.

THE IVAN A. GETTING LABORATORIES

The Laboratory Operations of The Aerospace Corporation is conducting experimental and theoretical investigations necessary for the evaluation and application of scientific advances to new military concepts and systems. Versatility and flexibility have been developed to a high degree by the laboratory personnel in dealing with the many problems encountered in the nation's rapidly developing space and missile systems. Expertise in the latest scientific developments is vital to the accomplishment of tasks related to these problems. The laboratories that contribute to this research are:

Aerophysics Laboratory: Launch and reentry aerodynamics, heat transfer, reentry physics, chemical kinetics, structural mechanics, flight dynamics, atmospheric pollution, and high-power gas lasers.

Chemistry and Physics Laboratory: Atmospheric reactions and atmospheric optics, chemical reactions in polluted atmospheres, chemical reactions of excited species in rocket plumes, chemical thermodynamics, plasma and laser-induced reactions, laser chemistry, propulsion chemistry, space vacuum and radiation effects on materials, lubrication and surface phenomena, photosensitive materials and sensors, high precision laser ranging, and the application of physics and chemistry to problems of law enforcement and biomedicine.

Electronics Research Laboratory: Electromagnetic theory, devices, and propagation phenomena, including plasma electromagnetics; quantum electronics, lasers, and electro-optics; communication sciences, applied electronics, semiconducting, superconducting, and crystal device physics, optical and acoustical imaging; atmospheric pollution; millimeter wave and far-infrared technology.

Materials Sciences Laboratory: Development of new materials; metal matrix composites and new forms of carbon; test and evaluation of graphite and ceramics in reentry; spacecraft materials and electronic components in nuclear weapons environment; application of fracture mechanics to stress corrosion and fatigue-induced fractures in structural metals.

Space Sciences Laboratory: Atmospheric and ionospheric physics, radiation from the atmosphere, density and composition of the atmosphere, aurorae and airglow; magnetospheric physics, cosmic rays, generation and propagation of plasma waves in the magnetosphere; solar physics, studies of solar magnetic fields; space astronomy, x-ray astronomy; the effects of nuclear explosions, magnetic storms, and solar activity on the earth's atmosphere, ionosphere, and magnetosphere; the effects of optical, electromagnetic, and particulate radiations in space on space systems.

THE AEROSPACE CORPORATION
El Segundo, California